Proceedings of the 21st ICSMGE, Vienna, Austria, 14 – 19 June 2026. Pistrol, Adam & Schweiger (eds.)
Published by: ÖGG, Austrian Society for Geomechanics, Salzburg, Austria, ISBN 978-3-9503898-4-5
https://doi.org/10.53243/ICSMGE2026-2085

Subsurface investigation of key liquefaction areas in İskenderun following the 2023 Kahramanmaraş earthquake

Cody Arnold
Geosyntec Consultants, Inc., Kennesaw, Georgia, USA, cody.arnold@geosyntec.com

Jorge Macedo
School of Civil and Environmental Engineering, Georgia Institute of Technology, Atlanta, USA

Jonathan D. Bray
Department of Civil and Environmental Engineering, University of California-Berkeley, Berkeley, USA

Diane Moug
Department of Civil and Environmental Engineering, Portland State University, Portland, USA

Fikret Atalay
EGSci Consulting, Atlanta, GA, USA

Patrick Bassal
Department of Civil, Environmental, and Geodetic Engineering, The Ohio State University, Columbus, OH, USA

Chenying Liu
School of Civil and Environmental Engineering, Georgia Institute of Technology, Atlanta, USA

Murat Bikçe
İskenderun Technical University, İskenderun, Hatay, Türkiye

Turan Durgunoğlu
Zemin Etüd ve Tasarım A.Ş. Istanbul, Türkiye

ABSTRACT: Key insights from a comprehensive subsurface investigation in the port city of İskenderun following the 2023 Mw 7.8 Kahramanmaraş earthquake are shared. The subsurface characterization was performed at sites experiencing notable liquefaction-induced damage using 40 cone penetration tests (CPTu) and 7 seismic CPTu (SCPTu). Subsurface profiles within the reclaimed shoreline area reveal consistent conditions, with dense gravelly fill underlain by a thick deposit of saturated sand and silty sand prone to liquefaction, which is then underlain by medium stiff-to-stiff clay. Comparatively, areas located within the historic inland boundary showed greater variability in the presence of gravel fill as well as the thickness and characteristics of the underlying sand and silty sand. Reclaimed shoreline areas experienced more severe liquefaction effects, including building settlements ranging from 22 cm to 74 cm, while historic inland zones showed reduced liquefaction susceptibility and lower settlements ranging from 0 cm to 50 cm. Additionally, site characterization using SCPTu near a critical strong motion station provides valuable ground characterization insights for seismic response evaluation in İskenderun. These findings, along with previously published post-event field observations, contribute to the development of high-quality field case histories that are essential for refining liquefaction assessment methods and the effects of liquefaction. Liquefaction manifestations and critical layer interpretations are delineated for advancing liquefaction-triggering assessments.

KEYWORDS: case histories, earthquake, liquefaction, settlement, site characterization.

1 INTRODUCTION

The 2023 Kahramanmaraş earthquake sequence caused widespread destruction across southeastern Türkiye, resulting in the loss of tens of thousands of lives. Evidence of significant liquefaction-related damage was identified by teams of the National Science Foundation (NSF)-supported Geotechnical Extreme Events Reconnaissance (GEER) Association in collaboration with researchers from Middle East Technical University (METU), Zemin Etüd ve Tasarım A.Ş. engineers, and other local engineers. Documentation of this liquefaction-related damage is provided in Cetin et al. (2023) and Moug et al. (2023). Further post-earthquake field observations in İskenderun are detailed in Moug et al. (2024a) and Bassal et al. (2024), which document liquefaction-induced impacts on 26 buildings and 7 transects affected by lateral spreading.

Post-earthquake reconnaissance following the moment magnitude (M_w) 7.8 Kahramanmaraş earthquake offered a valuable opportunity to develop a series of high-quality field case histories of liquefaction-induced damage in İskenderun, Türkiye. These case histories are presented in Arnold et al. (2025), Moug et al. (2024a), and Bassal et al. (2024). They contribute to the growing body of well-documented field data that play a critical role in the advancement and validation of procedures for evaluating both liquefaction triggering and its consequences. The cone penetration test (CPTu) was employed as the primary method for subsurface characterization, given its status as the preferred approach for liquefaction case histories in sandy soils due to its continuous data collection, precision, and reliability.

This study presents selected findings from CPTu investigations conducted in March 2024 as part of a broader

effort to document liquefaction-induced damage in İskenderun, Türkiye. The full dataset, including CPTu and SCPTu tests, ground motion estimates, and comprehensive analyses of lateral spreading and settlement, is detailed in Arnold et al. (2025). A total of 40 CPTu and 7 seismic CPTu (SCPTu) were performed to characterize subsurface conditions at sites affected by liquefaction. This paper highlights a subset of the building settlement case histories, focusing on representative examples that demonstrate the range of subsurface conditions present in İskenderun from the broader dataset. Subsurface conditions are documented at buildings that experienced liquefaction-induced settlements ranging from less than 6 cm to 51 cm. Additionally, the subsurface conditions at a local strong motion station (SMS) are also shown. CPTu-based evaluations of liquefaction triggering and post-liquefaction volumetric settlement are presented for selected sites using procedures commonly applied in engineering practice. All geo-located field-test electronic and meta data reported in this study are available at DesignSafe (Macedo et al., 2025).

2 LIQUEFACTION ASSESSMENT PROCEDURES

In this study, the CPTu-based liquefaction triggering procedure proposed by Boulanger and Idriss (2014) is used to calculate the factor of safety against liquefaction triggering (FS_{liq}). Soils susceptible to liquefaction are identified based on the soil behavior type index (I_c; Robertson and Wride, 1998), using a threshold value of $I_c \leq 2.6$. To assess the sensitivity of this threshold, a range of I_c values from 2.5 to 2.7 is evaluated. The influence of this variation on the identification of liquefiable layers and liquefaction indices is generally within 10% of the results obtained using the I_c of 2.6 threshold. One-dimensional (1D) free-field post-liquefaction volumetric reconsolidation settlement (S_v) is estimated using the method of Zhang et al. (2002). For building settlement sites, the liquefaction severity number (LSN) is calculated using van Ballegooy (2014), the liquefaction demand parameter L_D is calculated using Hutabarat and Bray (2022), which can be used to estimate ejecta-induced settlement using Bray and Olaya (2023), and the liquefaction building settlement index (LBS) is calculated using Bray and Macedo (2017). Ground motion intensity parameters (i.e., PGA, Sa(1s), and CAV) were estimated from recorded ground motions and a Kriging approach detailed in Arnold et al. (2025). Their reported range of median estimates within coastal İskenderun are 0.32 - 0.33 for PGA, 0.64 - 0.66 for Sa(1s), and 26 for CAV.

3 GEOLOGICAL AND TECTONIC SETTING

İskenderun is located in Hatay province in southeastern Türkiye, positioned on an alluvial plain between the Nur Mountains and the Mediterranean Sea. This area lies at the intersection of several tectonic plates and is part of the East Anatolian Fault Zone (EAFZ). On February 6, 2023, Türkiye experienced two major left-lateral earthquake events along the EAFZ. The first event had a moment magnitude (M_w) of 7.8 and occurred in the Pazarcık section of the EAFZ. The second event had an M_w of 7.5 and occurred nine hours later along the Çardakand Doğanşehir faults within the EAFZ. As shown in Figure 1, the first event ruptured along a northeast-southwest alignment, and the second event along a west-northeast alignment. The M_w 7.8 and M_w 7.5 earthquakes had focal depths of 8.6 km and 7.0 km, respectively. Figure 1 also shows the relative locations of these fault ruptures to İskenderun. Liquefaction in İskenderun was governed by the closer M_w 7.8 Pazarcık earthquake.

Much of İskenderun lies near sea level and has a history of both flooding and seismic activity. Historical descriptions of the area as swampy suggest high groundwater levels and poor drainage conditions. Urban development in the 20th century included shoreline reclamation through drainage and fill efforts (Nalça, 2018). The extent of the reclaimed shoreline was interpreted from historical (mid-1800s and early 1900s) maps (Nalça, 2018) by Moug et al. (2024a), who noted that its boundary closely aligns with Atatürk Boulevard, a major roadway in the city. Most liquefaction manifestations from the 2023 Kahramanmaraş earthquakes were observed within these filled areas (Moug et al., 2024a; Taftsoglou et al., 2023; Cetin et al., 2023; Moug et al., 2023). South of the Atatürk Boulevard, ejecta were generally limited, except in the Çay District, where the reclaimed zone extends farther inland. Regional subsurface studies indicate sandy surface sediments overlying silty and muddy layers to depths of 40–70 m (Eryılmaz and Eryılmaz, 2003; Özdemir et al., 2019), although these investigations did not include the reclaimed zone. A microzonation study by Denge Mühendislik Ltd. Sti. (2011) identified sands, gravels, silts, and clays to 30 m depth, with sand content increasing toward the shoreline and groundwater levels observed as shallow as 1.4 to 2 m near the coast.

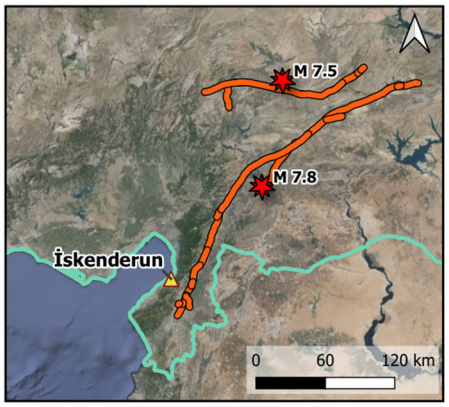

Figure 1. Locations of event faults (Reitman et al., 2023) and epicenters and İskenderun (Base map: Google, n.d.).

4 STUDY AREAS AND SITE INVESTIGATION OVERVIEW

Arnold et al. (2025) documented subsurface conditions at 17 building settlement sites, 7 lateral spread transects, and a critical SMS station close to the city. This study will highlight a selection of these sites to showcase the varying ground conditions within the reclaimed shoreline and the historic shoreline boundary, which are shown in Figure 2. Subsurface conditions from a local SMS station are also shown and provide valuable insights for regional seismic response evaluation.

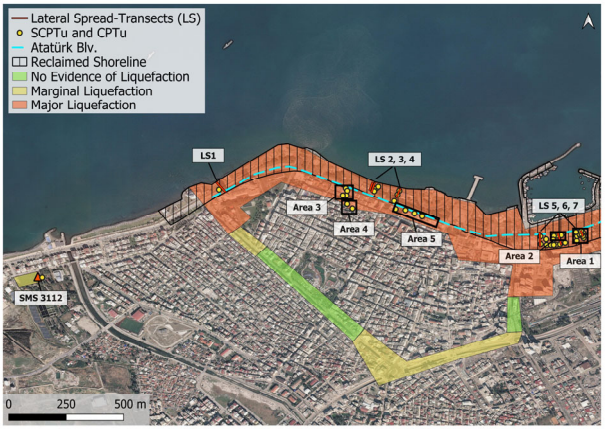

Figure 2. Overview of İskenderun study areas with demarcation of reclaimed and historic shoreline boundaries from Arnold et al. (2025).

Most CPTu required pre-drilling to depths between 1.5 and 4.5 m to penetrate dense upper gravelly fill layers encountered in the investigation areas. The resistance to drilling and CPTu advancement indicated these fills were dense. Standard penetration test (SPT) data reported by Özener et al. (2024) show a median overburden-corrected blow count $(N_1)_{60}$ of 30 in the gravelly fill, based on energy corrections derived by comparing SPT results in sand with CPTu data from this study. Most CPTu extended to depths of 30 m, with a few reaching as deep as 43.5 m.

Groundwater levels (GWL) were measured in the pre-drilled holes, and porewater dissipation tests were conducted at selected depths to verify the GWL and to obtain dissipation data. In most areas, the measured GWL was close to 1 m; however, accounting for post-earthquake settlement, the pre-event GWL is estimated at approximately 1.5 m, consistent with observations in Denge Mühendislik Ltd. Sti. (2011). This estimated depth of 1.5 m is used in the subsequent analyses.

4.1 *Seismic station TK-3112*

Seismic station TK-3112 is located 2 km west of the Çay District of İskenderun (Figure 2). Of the nearby seismic stations, TK-3112 is at a site most representative of the subsurface conditions in the study areas. Unfortunately, the recording at TK-3112 stopped early during the M_w 7.8 event, likely before the strongest shaking, so response spectra are not available for this station. A SCPTu was advanced at TK-3112 to capture its subsurface conditions and the V_s profile shown in Figure 3.

The SCPTu profile at SMS 3112 is shown in Figure 3. A thin, very stiff surface layer is present to a depth of approximately 1.2 m, likely representing construction debris due to its shallow depth and limited thickness. Below this, a stratified silty-clayey layer extends to about 2.8 m, characterized by a normalized friction ratio (F_r) fluctuating between 1% and 10%. This unit is underlain by a medium dense sand layer with a normalized cone resistance (Q_{tn}; Robertson, 2009) ranging from 130 to 150, which extends to a depth of roughly 4 m. A stiff gravelly sand to sand layer is encountered between 4 and 5 m ($Q_{tn} \geq 400$; F_r near 0.5%), followed by loose to medium dense sands and silty sands ($50 < Q_{tn} < 100$) extending to approximately 14.5 m. Clay ($I_c > 3$) with $Q_{tn} \leq 5$ and F_r around 2.5% extends from 14.5 m to the end of the sounding at 30 m. Seismic shear wave velocity (V_s) measurements indicate V_s values ≤ 200 m/s above 25 m depth, increasing to approximately 250 m/s by 30 m depth.

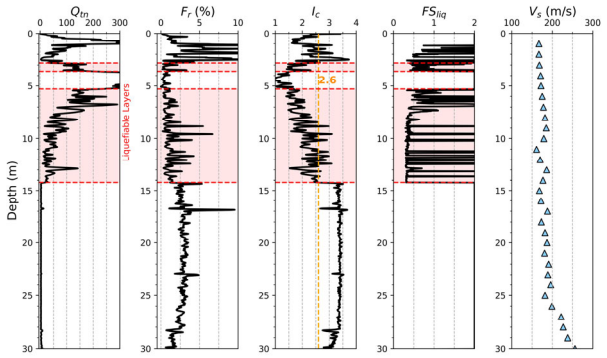

Figure 3. Normalized CPTu readings and V_s with calculated I_c and FS_{liq} at SMS 3112

4.2 *Area 2 settlement site*

Area 2 is located within the reclaimed shoreline in the Çay District (Figure 2). It includes three buildings: two reinforced concrete frame buildings with infill walls (RCF-IW) structures (Buildings K and M) and a one-story steel-frame building (Building L) situated between them on a concrete slab foundation (Figure 4). Buildings K and M are similar in construction to other structures in this area with salon-type first floors. Building M is a six-story structure with a partial seventh floor and a 2.5-m deep basement on a 30-cm thick slab. Building K is five stories tall and has a partial basement 2 m deep that does not span the full building footprint. Four CPTu and one SCPTu were performed at the corners of Buildings K and M along Atatürk Boulevard, with an additional CPTu placed at the rear corner of Building M (Figure 4). All CPTu were pre-drilled to 3 m to bypass dense gravelly fill.

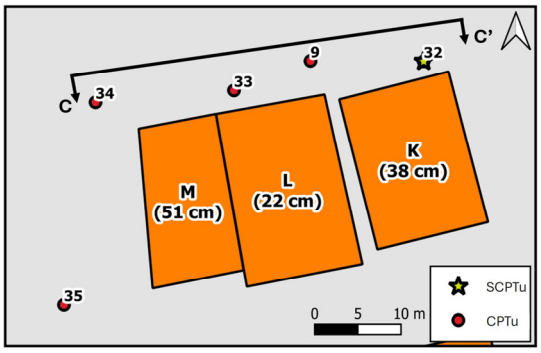

Figure 4. Overview of Area 2 site investigation from Arnold et al. (2025) with observed building settlements from Moug et al. (2024a).

As shown in the CPTu profiles in Figure 5, a sand layer beneath the fill and to approximately 10.8 m depth exhibits Q_{tn} values ranging from 75 to 120 and an I_c of approximately 1.8. Below the sand, an interbedded sandy silt and silty clay unit to 16 m depth contains thin liquefiable layers, with higher I_c values and lower Q_{tn} (≤ 30). A deeper clay unit is characterized by $Q_{tn} \leq 15$ and $I_c \geq 3$.

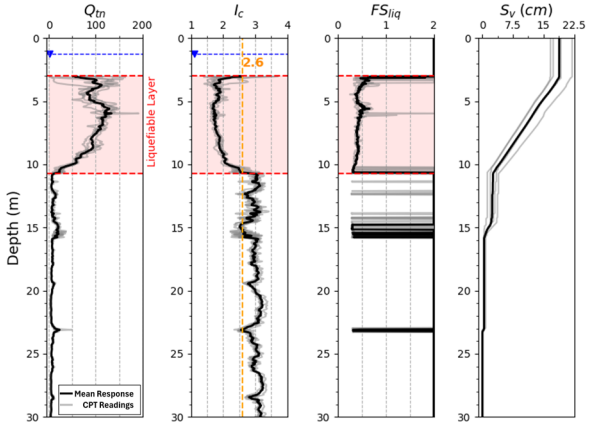

Figure 5. Normalized CPTu readings with calculated I_c, S_v, and FS_{liq} at Area 2 settlement site

The estimated S_v values for Area 2 range from 17 to 22 cm, as shown in Figure 5. The 16% to 84% ranges for LBS, LSN, and L_D are 23 to 31, 27 to 30, and 55 to 110, respectively. These values are consistent with those observed in other sites within the Çay District, as documented in Arnold et al. (2025).

4.3 *Area 4 settlement site*

Area 4 is located just south of Atatürk Boulevard, as shown in Figure 2, and lies within the historic shoreline (i.e., outside the reclaimed land). Liquefaction-induced settlement was observed at a single 5-story building (Building W), constructed on a 50-cm thick RC slab. The building has an empty lot to its northwest and an adjacent structure to the southeast. Building W settled only 6 cm, which is substantially less than similarly sized

buildings within the reclaimed shoreline (Arnold et al., 2025). Building W and the CPTu for Area 4 are shown in Figure 6. Two CPTu were performed to characterize subsurface conditions at this site: one on the southwest corner (CPTu 42) and another offset approximately 15 m from the southeast corner (CPTu 41) due to access constraints. Both CPTu required 1.5 m of pre-drilling, consistent with the thinner fill layers observed outside the reclaimed zone.

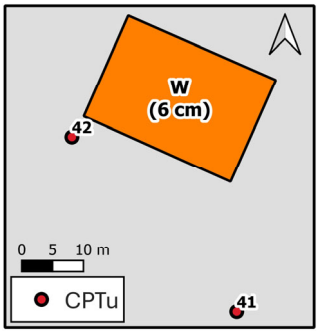

Figure 6. Overview of Area 4 site investigation from Arnold et al. (2025) with observed building settlements from Moug et al. (2024a).

The subsurface profile in Area 4 (Figure 7) includes a dense sand layer ($Q_{tn} \geq 150$) to a depth of 4 m, underlain by a looser sandy layer extending to approximately 14 m. The looser sandy layer exhibits Q_{tn} values generally ranging from 50 to 120 and I_c values less than 2.6, indicating susceptibility to liquefaction. Below this, a clay unit with $I_c > 3$ and low Q_{tn} values (< 15) extends to the end of the sounding at 30 m. The liquefiable sandy layer is thicker than that observed in Area 2.

FS_{liq} is below 1 for much of the upper 14 m (Figure 7). The values of L_D (42 and 88) indicate severe ejecta potential, which is consistent with other areas. The values of S_v (23 and 27 cm), LBS (34 and 39), and LSN (28 and 34) calculated for the 2 CPTu in Area 4 are also relatively consistent with other areas (Arnold et al., 2025). Despite the presence of a thick liquefiable layer, the relatively low observed settlement of Building W is an important observation that warrants further study.

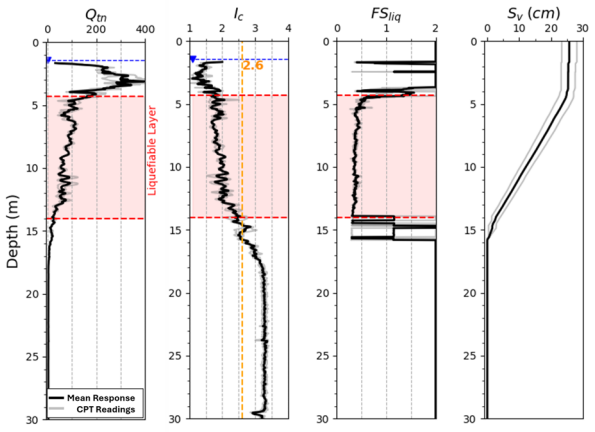

Figure 7. Normalized CPTu readings with calculated I_c, S_v, and FS_{liq} at Area 4 settlement site

4.4 *Area 5 settlement site*

Area 5 includes six buildings (S, R, Q, P, O, and N) situated along Atatürk Boulevard (the boundary between reclaimed land and historic shoreline) between Areas 2 and 4, as shown in Figure 2. Building plans for this area were not available. Buildings S, Q, and N are seven-story structures; Buildings O and R are smaller, with six and five stories, respectively; and Building P is a historic two-story building (Moug et al., 2024).

Four CPTu were performed to assess the subsurface conditions in this area, shown in Figure 8. CPTu 43, 44, and 46 were pre-drilled to depths of 1.5 m, while CPTu 12 required 3 m of pre-drilling. As shown in Figure 9, the CPTu responses in Area 5 are somewhat consistent with those in Area 4, though the liquefiable sandy layer is slightly thicker, due to the upper dense sandy layer only extending to a depth of 3 m.

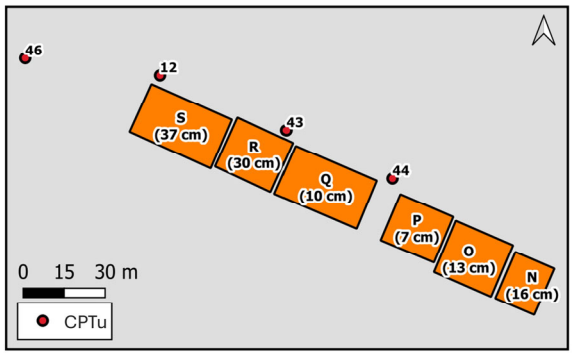

Figure 8. Overview of Area 5 site investigation from Arnold et al. (2025) with observed building settlements from Moug et al. (2024a).

The representative CPTu profile (Figure 9) shows a dense sandy layer ($Q_{tn} \geq 200$) extending to a depth of 3 m; however, this layer is not present in CPTu 44. Underneath is a thick sandy layer extending to about 14 m. This sandy unit exhibits Q_{tn} values between 50 and 110 and I_c values below 2.6, indicating liquefiable material. FS_{liq} is less than 1 throughout this depth range, and S_v is estimated to be approximately 27 cm, except for CPTu 44, which has a larger estimate of 32 cm due to the absence of a stiffer upper sand layer. Below the liquefiable zone, a clay unit with Q_{tn} less than 15 and I_c greater than 3 is present to the bottom of the sounding at 30 m.

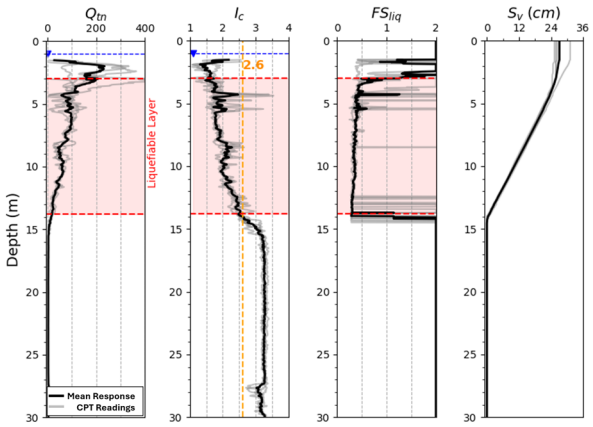

Figure 9. Normalized CPTu readings with calculated I_c, S_v, and FS_{liq} at Area 5 settlement site

The overall ranges of S_v (25 to 32 cm), LBS (40 to 62), LSN (33 to 53), and L_D (60 to 90) in Area 5 are generally higher than the values observed in Areas 2 and 4. However, the buildings in Area 5 exhibited a wider range of settlements between 7 and 37 cm. Buildings Q, O, and N experienced significantly less settlement than Buildings S and R, despite CPTu 44, located closest to Buildings Q, O, and N, indicating higher S_v, LBS, and LSN values. This discrepancy may be attributed to factors such as differences in structural design, including foundations or basements, which remain unknown but should be explored in future studies.

5 DISCUSSION

The subsurface investigation reveals that conditions along the İskenderun shoreline are similar, with some important variations. CPTu in Area 2 located within the eastern portion of the reclaimed shoreline (i.e., Çay district) required deeper pre-drilling (3 m) compared to Area 4 (1.5 m). Area 5 is unique in that it lies on the boundary between the historic shoreline and reclaimed land (i.e., Atatürk Boulevard) and had variable amounts of gravelly fill, with most CPTu requiring 1.5 m of pre-drilling, except for CPTu 12, which required 3 m. Despite 3 m of pre-drilling being indicative of reclaimed land, the CPTu responses for Area 5 (Figure 9) align more closely with those in Area 4 (Figure 7) than with those in Area 2 (Figure 5), suggesting that it lies within the historic shoreline. This highlights some inconsistency in the gravelly fill along the historic shoreline.

The general CPTu response indicates a predominantly sandy layer with I_c values between 1.3 and 2.2 across the investigation area. This layer is relatively uniform within the reclaimed land but appears denser in areas within the historic shoreline (e.g., SMS 3112 and Area 4). In the eastern reclaimed zone (e.g., Area 2 and the Çay District), the sand is underlain by interbedded sandy silts and clayey silts, transitioning into more uniform silty clay with thin silt or sand seams. In the western reclaimed area (e.g., Area 5), the upper sand layer thickens to approximately 14 m and transitions directly to clay, with little-to-no interbedded zone observed. Within the historic land boundary, CPTu show denser sandy silt to sand in the upper 3 m, followed by sand to silty sand to about 15 m depth, underlain by silt and clay units.

5.1 *Performance of CPTu liquefaction indices at building settlement sites*

The CPTu-based liquefaction indices presented in this study (e.g., S_v, LBS, LSN, and L_D) are for preliminary assessment to support the subsurface characterization of key areas in İskenderun. Detailed back analyses are needed to fully assess their performance. While acknowledging this, a comparison of performance to field observations is still insightful. To facilitate this, Table 1 summarizes the previously reported indices for selected building sites (see Appendix A in Arnold et al., 2025 for more details). In Area 5, the easternmost CPTu (CPTu 44) lacks the dense upper sand layer ($Q_{tn} \geq 200$) observed in the three western CPTu (CPTu 46, 12, and 43). As a result, Area 5 is subdivided into Sites 5A (CPTu 46, 12, and 43) and 5B (CPTu 44).

Table 1. Summary of liquefaction indices at selected building settlement sites (16% - 84% values for Areas with more than 2 CPTu)

Site	S_v (cm)	LBS	LSN	L_D
Area 2	15–22	23–31	27–30	55–110
Area 4	23 & 27	34 & 39	28 & 34	42 & 88
Area 5A	25–26	40–62	33–39	60–90
Area 5B	32	49	53	73

Considering the estimated indices in Table 1 with measured settlements (Figure 4, Figure 7, and Figure 9) and observations of ejecta (Moug et al., 2023; Cetin et al., 2023; Moug et al., 2024a), some patterns emerge. In Area 2, high indices correspond with both large building settlements and significant ejecta. In Area 4, high indices are present but do not align with the low building settlement and lack of ejecta. Area 5A shows alignment between high indices, significant building settlements (Buildings S and R), and significant ejecta. In contrast, Area 5B also has high index values, but these are not reflected in the low building settlements (Buildings Q, P, O, and N), though significant ejecta was observed. These variations could be contributed to differences in construction (e.g., foundation type and basement) or adjacent building settlement interactions (Moug et al. 2024).

5.2 *Critical layers for liquefaction assessments*

Arnold et al. (2025) interpreted and summarized critical layer properties for level-ground sites in İskenderun. Table 2 lists the critical layers identified at the selected sites presented in this study. Due to space limitations, only a subset of the interpreted properties is shown; readers are referred to Arnold et al. (2025) for the full dataset and discussion.

Table 2. Critical layers determined for selected level ground sites

Site	Liquefaction Manifestation	Depth Interval (m)	Geomean Q_{tn}	Geomean I_c
Area 2	*Yes*	3.3–5.0	90	1.83
Area 4	*Yes*	4.3–9.0	101	1.79
Area 5A	*Yes*	3.8–7.0	96	1.81
Area 5B	*Yes*	2.0–3.3	86	1.73
SMS 3112	*No*	2.9–3.5	133	1.69

The İskenderun level-ground case histories are well-constrained by the seismic demand of the M_w 7.8 Pazarcık earthquake, supported by ground motion recordings, CPTu soundings, and surface evidence of liquefaction (i.e., ejecta). The critical layer at each site was identified using the approach of Dhakal et al. (2020), which is similar to that of Green et al. (2014). The critical layer is defined as the soil layer most likely to have liquefied early in the shaking and produced visible surface manifestations. At the investigated sites, thick sand to silty sand units are interpreted to have liquefied, as shown in Figure 3, Figure 5, Figure 7, and Figure 9. Within these units, the critical layer was selected as the weakest and shallowest zone of sufficient thickness to produce ejecta. Profiles of Q_{tn}, I_c, FS_{liq}, and S_v (e.g., Figure 9) were used to guide this selection, with critical layers typically exhibiting consistent penetration resistance and I_c values.

The information provided in Table 2 and those in Arnold et al. (2025) may be useful for future efforts involving evaluation of liquefaction triggering procedures, site response analyses, and effective stress soil-structure interaction modeling at the building sites presented in this study.

6 CONCLUSIONS

The 2023 M_w 7.8 Pazarcık earthquake caused extensive liquefaction-related damage in the port city of İskenderun. A focused field investigation using 40 CPTu and 7 SCPTu was conducted to characterize subsurface conditions at several building settlement sites and one seismic monitoring station surveyed after the earthquake. The subsurface profile along the historic shoreline and within the reclaimed shoreline area was found to be relatively consistent, with a dense gravelly fill overlying a thick deposit of liquefiable sand. In the Çay District, this sand layer is underlain by an interbedded zone of silt and sand, which then transitions into a thick clay layer. In other areas, the sand transitions directly into the clay layer with little to no presence of the interbedded zone.

A subset of the building settlement sites, along with the geotechnical characterization of the seismic station, are discussed in this paper. The full dataset, including lateral spread transects, estimated ground motion intensity measures such as PGA, CAV, and Sa(1s), and detailed liquefaction assessment results, is presented in Arnold et al. (2025). That study

integrates these data with observed ground and building deformations from Moug et al. (2024a) and Bassal et al. (2024) to develop high-quality liquefaction field case histories in İskenderun.

Although sandy layers susceptible to liquefaction were commonly identified across the reclaimed shoreline, the resulting building settlements varied significantly, from less than 6 cm to 51 cm. The case histories provide useful data for evaluating and refining liquefaction triggering and consequence models. Summaries of critical layer properties and liquefaction manifestations contribute to ongoing efforts to improve empirical procedures and support the development of more robust analytical approaches.

7 ACKNOWLEDGEMENTS

This research is supported by the NSF through the Engineering for Civil Infrastructure Program under Grant No. CMMI 23380-23, -24, -25, -26. It also takes advantage of data collected through the NSF-supported GEER Association under Grant No. CMMI1826118. Any opinions, findings, conclusions, or recommendations expressed in this material are those of the authors and do not necessarily reflect the views of the NSF. Any use of trade, firm, or product names is for descriptive purposes only and does not imply endorsement by the U.S. Government. Researchers from the Middle East Technical University received support from the Turkish government. The fieldwork was conducted in coordination with Zemin Etüd ve Tasarım A.Ş. A GEER team member, Sena Begüm Kendir, and Dr. H. Turan Durgunoğlu provided guidance and logistical support to the team. We also sincerely thank T.C. Antakya Kaymakamlığı for their valuable assistance and support.

8 DATA AVAILABILITY STATEMENT

Some or all the data on post-event observations included in this publication are available at DesignSafe DOI: https://doi.org/10.17603/ds2-q5x1-e497 (Moug et al., 2024b). Additionally, all geo-located field-testing data reported in this study are available at DesignSafe DOI: https://doi.org/10.17603/ds2-6473-fs88 (Macedo et al., 2025).

9 REFERENCES

Arnold, C., Macedo, J., Bray, J.D., Moug, D., Atalay, F., Bassal, P., Liu, C., Bikçe, M., and Durgunoğlu, T. 2025. Field Characterization of Areas in İskenderun Affected by Liquefaction during the 2023 Kahramanmaraş Earthquake. *Earthquake Spectra*.

Bassal, P., Papageorgiou, E., Moug, D., Bray, J., Cetin, K., Şahin, A., Kubatko, E., Nepal, S., Toth, C., Kendır, S., and Bikce, M. 2024. Liquefaction ground deformations and cascading coastal flood hazard in the 2023 Kahramanmaraş earthquake sequence. *Earthquake Spectra* 40 (3).

Boulanger, R., and Idriss, I. 2014. CPT and SPT based liquefaction triggering procedures, report no: UCD/CGM-14/01. *Center for Geotechnical Modeling*, University of California, Davis.

Bray, J., and Macedo, J. 2017. 6th Ishihara lecture: Simplified procedure for estimating liquefaction induced building settlement. *Soil Dynamics and Earthquake Engineering* 102, 215–231.

Bray, J.D., and Olaya, F.R. 2023. 2022 H. Bolton Seed Memorial Lecture: Evaluating Liquefaction Effects. *Journal of Geotechnical and Geoenvironmental Engineering* 149 (8).

Cetin, K., Bray, J., Frost, J., Hortacsu, A., Miranda, E., Moss, R., and Stewart, J. 2023. February 6, 2023 Türkiye earthquakes: Report on geoscience and engineering impacts. GEER Association Report 082, May 6. Oakland, CA: *Earthquake Engineering Research Institute*.

Dhakal, R., Cubrinovski, M., and Bray, J.D. 2020. Geotechnical Characterization and Liquefaction Evaluation of Gravelly Reclamations and Hydraulic Fills (Port of Wellington, New Zealand). *Soils and Foundations* 60, 1507–1531.

Denge Mühendislik Ltd. Sti. 2011. Hatay Ili - Iskenderun Ilcesi - Iskenderun Belediyesi Mikrobolgeleme Etud Raporu.

Eryılmaz, M., and Eryılmaz, F.Y. 2003. Recent Surface Sediment Distribution of Iskenderun Bay. *Proceedings of 56th Geological Congress of Turkey*, 286–287.

Google (n.d.). Southeastern Türkiye. [Online] Available at : https://mt1.google.com/vt/lyrs=s\&x={x}\&y={y}\&z={z}. [Retrieved March 12, 2024].

Green, R.A., Cubrinovski, M., Cox, B., Wood, C., Wotherspoon, L., Bradley, B., and Maurer, B. 2014. Select liquefaction case histories from the 2010–2011 Canterbury earthquake sequence. *Earthquake Spectra* 30, 131–153.

Hutabarat, D., and Bray, J. 2022. Estimating the Severity of Liquefaction Ejecta Using the Cone Penetration Test. *Journal of Geotechnical and Geoenvironmental Engineering* 148.

Macedo, J., Bray, J., Moug, D., Bassal, P., and Arnold, C. 2025. Subsurface Characterization of Iskenderun - 2024 in Subsurface Characterization of Selected Liquefaction Case Histories - 2023 Kahramanmaras Earthquake Sequence. DesignSafe-CI. https://doi.org/10.17603/ds2-6473-fs88

Moug, D., Bassal, P., Bray, J., Cetin, K., Kendir, S., Şahin, A., Cakir, E., Soylemez, B., and Ocak, S. 2023. February 6, 2023 Türkiye earthquakes: GEER phase 3 team report on selected geotechnical engineering effects. *GEER Association Report 082-S1*, June 30. Ankara: Middle East Technical University.

Moug, D., Bray, J., Bassal, P., Macedo, J., Ulmer, K., Cetin, K., Kendir, S., Şahin, A., Arnold, C., and Bikçe, M. 2024a. Liquefaction-induced ground and building interactions in İskenderun from the 2023 Kahramanmaraş earthquake sequence. *Earthquake Spectra*, 40(2), 913–938.

Moug, D., Bray, J., Bassal, P., Şahin, A., and Kendır, S. 2024b. Lidar Scans of Liquefaction-Impacted Buildings in İskenderun, Hatay in GEER Lidar Data from the 2023 Kahramanmaras Earthquake Sequence Reconnaissance. DesignSafe-CI. https://doi.org/10.17603/ds2-q5x1-e497

Reitman, N., Briggs, R., Barnhart, W., Jobe, J., DuRoss, C., Hatem, A., Gold, R., Mejstrik, J., and Akçiz, S. 2023. Preliminary fault rupture mapping of the 2023 Mw7.8 and Mw7.5 Türkiye earthquakes.

Nalça, C. 2018. Transformation of Iskenderun historic urban fabric from mid-19th century to the end of the French mandate period. M.S. thesis, Department of Architectural Restoration, Izmir Institute of Technology, Izmir, Turkey.

Özdemir, A., Yasxar, E., and Şahinoglu, A. (2019). \textit{Geothermal geophysical studies in Iskenderun (Hatay): The first indication for geothermal energy.} Proceedings of the 3rd International Symposium on Multidisciplinary Studies and Innovative Technologies.

Özener, P., Monkul, M.M., Bayat, E.E., Ari, A., and Cetin, K.O. 2024. Liquefaction and performance of foundation systems in Iskenderun during 2023 Kahramanmaras-Turkiye earthquake sequence. *Soil Dynamics and Earthquake Engineering*, 178.

Robertson, P.K., and Wride, C.E. 1998. Evaluating cyclic liquefaction potential using the cone penetration test. *Canadian Geotechnical Journal* 35(3), 442–459.

Robertson, P. 2009. Performance-based earthquake design using the CPT. In T. Kokusho, Y. Tsukamoto, and M. Yoshimine (Eds.), *Earthquake Geotechnical Engineering: From Case History to Practice*, 3–20. Taylor & Francis, London.

Taftsoglou, M., Valkaniotis, S., Papathanassiou, G., and Karantanellis, E. 2023. Satellite imagery for rapid detection of liquefaction surface manifestations: The case study of Türkiye-Syria 2023 earthquakes. *Remote Sensing*.

van Ballegooy, S., Malan, P., Lacrosse, V., Jacka, M., Cubrinovski, M., Bray, J., O'Rourke, T., Crawford, S., and Cowan, H. 2014. Assessment of liquefaction-induced land damage for residential Christchurch. *Earthquake Spectra* 30, 31–55.

Zhang, G., Robertson, P., and Brachman, R. 2002. Estimating liquefaction-induced ground settlements from CPT for level ground. *Canadian Geotechnical Journal* 39, 1168–1180.